Statistical Physics of Multimode Ordered and Disordered Lasers

F. Antenucci[1,2], **A. Crisanti**[1,3], **M. Ibáñez Berganza**[1,4], **and L. Leuzzi**[1,2]

[1]Dipartimento di Fisica, Università di Roma Sapienza, Piazzale A. Moro 2, Rome I-00185, Italy
[2]NANOTEC-CNR, Soft and Living Matter Lab, Piazzale A. Moro 2, Rome I-00185, Italy
[3]ISC-CNR, UOS Sapienza, Piazzale A. Moro 2, Rome I-00185, Italy
[4]INFN, Gruppo Collegato di Parma, via G.P. Usberti, Parma 7/A-43124, Italy

Abstract— The adoption of a statistical mechanical framework in optics provides realistic models for multimode laser systems, whose experimental implications are presented and critically analyzed. A model for passive mode locking lasers is analyzed beyond the mean-field approximation, accounting for the presence of many well-resolved frequencies of the lasing modes. The inhomogeneous structure in the nonlinear "mode locked" interaction network is shown to yield short pulses and phase waves with nontrivial slopes, corresponding to a phase delay of the pulsed laser signal. The analytic solution of a mean field-model for multimode laser in open and irregular cavities will be, afterwards, addressed. The complete phase diagram, in terms of degree of disorder, pumping rate of the source and strength of nonlinearity, consists of four different photonic regimes: incoherent fluorescence, mode locking, random lasing and the novel "phase locking wave". A replica symmetry breaking transition occurs at the random lasing threshold. For a high enough strength of nonlinearity, a whole region with nonvanishing complexity anticipates the transition and the light in the disordered medium displays typical glassy behavior.

1. STATISTICAL MECHANICS FOR MULTIMODE LASERS

There have been several studies addressing the description of multimode laser systems in a statistical mechanics framework [1–5]. The approach is based on the hypothesis of effective equilibrium. Lasers are manifestly off-equilibrium and energy is pumped into the system to sustain population inversion and stimulated emission. However, as the system power is kept constant, the resulting stationary regime can be described as if at equilibrium with an effective "thermal bath" whose "temperature" is related to the pumping rate and to the true environment temperature.

The evolution of the atom-field system operators can be formalized starting from the Jaynes-Cumming Hamiltonian for matter-light interaction. The system is localized in space with discrete states. If the optical resonator is open the system is embedded in a natural environment consisting of the continuum of extended scattering states. The coupling with the scattering states of the continuum determine the lifetime of the discrete states, which is, therefore, finite. Adopting, e.g., the system-and-bath approach [6], a rigorous quantization of the field is possible also when the cavity is not closed: contributions of radiative and localized modes are separated by Feshbach projection and an effective theory in the subspace of localized modes is obtained with an effective linear damping coupling.

Adopting the semiclassical limit and assuming that the mode lifetimes are much longer than the characteristic times of pump and loss, it is possible to adiabatically remove the atomic variables and obtain the (non-linear) equations for the field alone. The evolution in the lasing regime is then conveniently expressed in the basis of the *slow amplitude modes*. These are solutions $\bar{a}_k$ of angular frequencies ω_l with a harmonic form for long times $t \gg 1$. The mode evolution for the slow complex amplitudes $a_k(t) = \bar{a}_k(t)\, \mathrm{e}^{+\mathrm{i}\omega_k t}$ is, then, written as

$$\dot{a}_k = -\partial \mathcal{H}/\partial a_k^* \tag{1}$$

where, at the third order in the mode amplitude expansion, the functional $\mathcal{H}$ reads

$$\mathcal{H} = -\sum_{k=1,\dots N} G_k\, |a_k|^2 - \sum_{\mathbf{k}|\mathrm{FMC}(\mathbf{k})} J_{k_1 k_2}\, a_{k_1}^* a_{k_2} - \sum_{\mathbf{k}|\mathrm{FMC}(\mathbf{k})} J_{k_1 k_2 k_3 k_4}\, a_{k_1}\, a_{k_2}^* a_{k_3} a_{k_4}^*. \tag{2}$$

Here G_k is the gain curve of the active medium and the couplings between different modes are

$$J_{k_1 k_2} \propto \gamma_{k_1 k_2} - \int d\mathbf{r}\, \rho(\mathbf{r})\, g_l^*(\mathbf{r}) g_k(\mathbf{r}), \quad J_{k_1 k_2 k_3 k_4} \propto -\int d\mathbf{r}\, \rho(\mathbf{r}) g_l^*(\mathbf{r})\, g_{k_1}(\mathbf{r}) g_{k_2}^*(\mathbf{r})\, g_{k_3}(\mathbf{r})\,, \tag{3}$$

the matrix γ_{lk} being the damping matrix associated to the openness of the cavity [6] and $\rho(\mathbf{r})$ the density of atoms of the active medium.

In Eq. (2), by definition of slow amplitude mode $\bar{a}_l \simeq \mathrm{e}^{-\mathrm{i}\omega_k t}$, the sums are restricted to terms with different indices that meet the *frequency matching conditions* (FMC):

$$\text{linear: } |\omega_{k_1} - \omega_{k_2}| \lesssim \gamma \quad \text{nonlinear: } |\omega_{k_1} - \omega_{k_2} + \omega_{k_3} - \omega_{k_4}| \lesssim \gamma. \tag{4}$$

The finite line-width γ of the modes can be obtain only in a complete quantum derivation. In general, the linear term of Eq. (2) may have non-zero off-diagonal terms. They are all zero when the frequencies are well distinct so that the frequency matching condition of the linear term is never satisfied but for the modes with overlapping frequency. While this is generally true for standard high quality-factor lasers, for a random laser (RL) [7] there can be a significant frequency overlap between the lasing modes and off-diagonal linear contributions must be considered.

For a complete statistical description one must, eventually, consider the presence of the noise $F_l(t)$ in Eq. (1), linked primarily to spontaneous emission. Though, in general, non-diagonal, a proper mode basis can be chosen where F_l is white and uncorrelated:

$$\langle F^*_{k_1}(t_1)\, F_{k_2}(t_2)\rangle = 2T\delta_{k_1k_2}\delta(t_1 - t_2), \quad \langle F_{k_1}(t_1) F_{k_2}(t_2)\rangle = 0, \tag{5}$$

with T being the spectral power of the noise, proportional to the heat-bath temperature.

The functional $\mathcal{H}$ in Eq. (2) is complex in the most general case. The real part is associated with a purely dissipative motion while the imaginary part with dispersion. Without dissipation, the total optical intensity $\mathcal{E}$ is a constant of motion. Differently, the system remains stable because the gain decreases as the optical intensity increases. To study the equilibrium properties, this can be encoded by requiring that at any instant gain and losses balance to keep $\mathcal{E}$ constant [1]:

$$\mathcal{E} = \epsilon N = \sum_{k=1,\dots N} |a_k|^2 = \text{const.} \tag{6}$$

Hereinafter we consider only purely dissipative systems. These can be studied using the standard tools of the equilibrium statistical physics: the Langevin equations Eq. (1) reduce to the potential form and, hence, the steady-state solution of the associated Fokker-Plank equation is the Gibbs distribution $\rho(a_1, \dots a_N) \propto \mathrm{e}^{-\mathcal{H}_R/T_{\mathrm{ph}}}$. The effective "photonic" temperature is taken $T_{\mathrm{ph}} = T/\epsilon^2 \equiv \mathcal{P}^{-2}$, proportional to the heat-bath temperature T and with $\mathcal{P}$ being the *pumping rate* of the source. This encodes the experimental observation that, regard to the lasing threshold, the effect of lowering T is equivalent to raise the optical intensity [8].

2. PASSIVE MODE LOCKING WITH FREQUENCY COMB

The model for passive mode locking lasers is obtained by the ordered limit of Eq. (2) [1–3]

$$\mathcal{H} = -\sum_{k=1,\dots N} G_k |a_k|^2 - \frac{J}{2} \sum_{\mathbf{k}|\mathrm{FMC}(\mathbf{k})} a_{k_1}\, a^*_{k_2} a_{k_3} a^*_{k_4}, \tag{7}$$

with the mode frequencies given by the frequency comb associated to the Fabry-Pérot resonator:

$$\omega_k = \ \omega_1 + (k-1)\Delta\omega, \quad k = 1, \dots, N. \tag{8}$$

The narrow-band, low finesse, limit $\gamma \simeq \Delta\omega$ is such that the FMC in Eq. (4) is always satisfied and can be solved in mean-field theory [1]. The FMC becomes nontrivial for high-finesse, $\gamma \ll \Delta\omega$. Monte Carlo simulations of both systems have been performed to study the role of FMC [2, 3].

In both low and high finesse cases, a first order transition is observed between a continuous wave regime at low pumping and a pulsed regime at high pumping. The critical pumping value being compatible, in the thermodynamic limit, with the one obtained in mean-field, cf. Fig. 1(a).

The difference between the high and low finesse cases is in the *nature* of the pulsed regime. For low finesse, the modes are trivially phase-locked $\phi_j = \phi_0$, so the parameter of global coherence $m_x \equiv \sum \Re(a_j)/N$ is nonzero, converging on the black line of in Fig. 1(b) for high pumping. In the high finesse case, instead, the pulsed regime is not trivially phase locked, see Fig. 1(b), and the laser mode phases result to behave as $\phi_j \simeq \phi_0 + \phi'\,\omega$, with a nontrivial, frequency independent, slope ϕ' (see insets in Fig. 2(a)). The slope ϕ' changes in the time evolution with a distribution

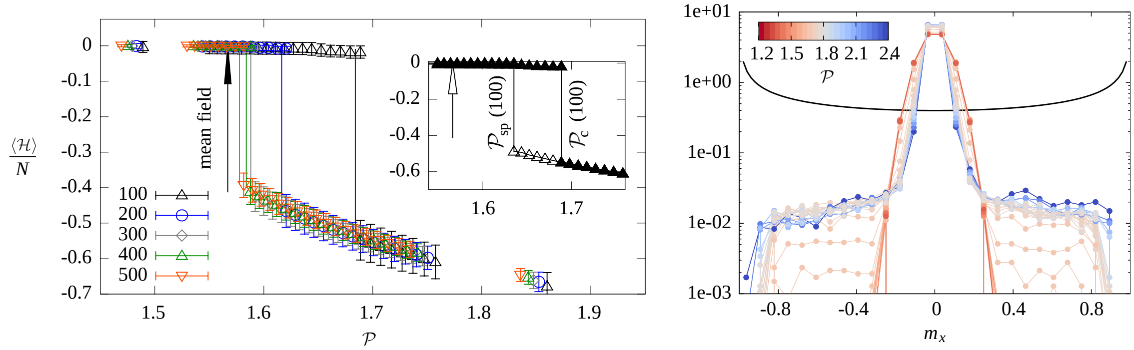

(a) (b)

Figure 1: (a) Intensive energy vs Pumping for high-finesse systems of increasing sizes. The inset shows the metastable region between the spinodal and critical line for $N = 100$. (b) Distribution of $m_x \equiv \sum \Re(a_j)/N$ for a high-finesse system with $N = 300$ at several pumping rates above and below the mode locking threshold. The solid black line is the distribution of m_x for a trivially phase locked system $\phi_j \equiv \phi_0$.

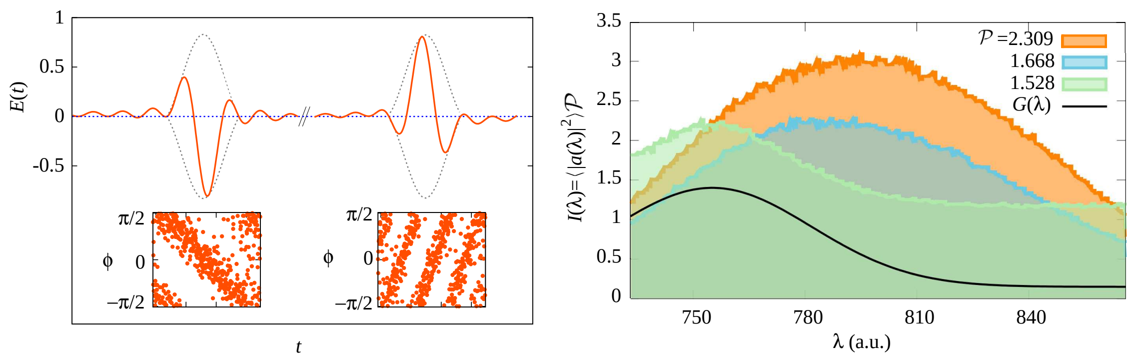

(a) (b)

Figure 2: (a) Signal (top) and corresponding configurations plotted as Phase vs Frequency (bottom) for a high finesse system with $N = 500$ just above the critical pumping ($\mathcal{P} = 1.692$, $\mathcal{P}_c = 1.565(8)$). (b) Intensity spectra for three pumping for high finesse and $N = 150$ ($\mathcal{P}_c = 1.60(2)$ here). Below the threshold the spectrum is shown to follow the gain curve (black solid line).

determined by the interaction network among the modes and with a lifetime that increases with the pumping rate [2, 3]. Consequently, all the two mode correlators are zero in the high pumping regime in high finesse systems [2, 3]. The electromagnetic pulse associated with such configurations, $E(t) = \sum_j |a_j| \exp[\mathrm{i}(\omega t + \phi_j)]$, is, accordingly, such that the phase delay between the carrier and the envelope of the signal changes at each shot, cf. Fig. 2(a). The phenomenon is observed also in high-finesse models with fixed intensities (XY and p-clock models) [2, 3, 9] and it is reminiscent of the properties of lattice gauge theories where local gauge symmetries forbid the global $O(2)$ symmetry breaking [2, 3].

The FMC results to play an essential role not only for the phase locking but for the intensity spectra as well. Indeed, for low pumping the spectrum follows the gain curve G_k. As the pumping exceeds the mode locking threshold, however, the spectrum is observed to be determined solely by the interaction network and it becomes narrow around the central frequencies of the bandwidth, cf. Fig. 2(b), because of the FMC. This furnishes a theoretical mechanism to explain the gain narrowing at the mode locking transition.

3. MEAN FIELD MODEL FOR NONLINEAR OPTICS IN RANDOM MEDIA

In the general case of RLs, the cavity is open, so the matrix $\gamma_{k_1 k_2}$ is nonzero [6], while the spatial distribution of the modes is irregular and complicated in such a way that the interactions in Eq. (3) take, in principle, a wide range of values, positive and negative. In the mean-field theory the FMC of Eq. (4) are neglected and the $J_{i_1,\ldots,i_p}$ are then taken as independent identically distributed random variables. This is exact, in particular, for systems with spatially extended modes and a narrow bandwidth. Here we take the distributions of $J_{i_1,\ldots,i_p}$ in Eq. (2) Gaussian with ($p = 2,\, 4$)

$$\mathcal{P}\left(J_{i_1\ldots i_p}\right) = \frac{1}{\sqrt{2\pi\sigma_p^2}} \exp\left[-\frac{\left(J_{i_1\ldots i_p} - \tilde{J}_0^{(p)}\right)^2}{2\sigma_p^2}\right] \quad \text{with} \quad \sigma_p^2 = \frac{J_p^2}{2N^{p-1}}, \quad \tilde{J}_0^{(p)} = \frac{J_0^{(p)}}{p!\,N^{p-1}}. \tag{9}$$

The scaling of σ_p and $\tilde{J}_0^{(p)}$ with N assures the extensivity of the Hamiltonian. To have a direct interpretation in terms of photonics quantities we use the photonic parameters

$$J_0^{(4)} = \alpha_0 J_0, \quad J_0^{(2)} = (1-\alpha_0)J_0, \quad R_J = \frac{J}{J_0}, \tag{10}$$

$$J_4^2 = \alpha^2 J^2, \quad J_2^2 = (1-\alpha)^2 J^2, \quad \mathcal{P} = \epsilon\sqrt{\beta J_0}\,. \tag{11}$$

The parameters J_0 and J fix, respectively, the cumulative strength of the ordered and disordered part of the Hamiltonian while α_0 and α the *strength of nonlinearity* in the ordered and disordered parts. The parameter R_J is the *degree of disorder*.

The model is solved by means of the replica method for disordered systems [10] and their relative order parameters, the overlaps (i.e., the similarities) between thermodynamic states. This is achieved considering n identical replicas of the system that act as probes exploring the phase space and evaluating the physical overlaps between states from the overlap between these replicas.

In this way one obtains the free energy as a function of generalized order parameters [4, 5]

$$r_d = \frac{1}{\mathcal{E}}\sum_{k=1}^{N}\Re\left[(a_k^{\mathsf{a}})^2\right], \quad m = \frac{\sqrt{2}}{N}\sum_{k=1}^{N} a_k^{\mathsf{a}}, \quad Q_{\mathsf{ab}} = \frac{1}{\mathcal{E}}\sum_{k=1}^{N}\Re\left[a_k^{\mathsf{a}}\left(a_k^{\mathsf{b}}\right)^*\right]. \tag{12}$$

Here r_d is the parameter of partial coherence, m is the complex parameter of global coherence and Q_{ab} is a real overlap matrix. A main point is that the simplest ansatz of assuming $Q_{\mathsf{ab}} = Q$ for all $\mathsf{a} \neq \mathsf{b}$, i.e., of assuming that all replicas are equivalent, is not consistent in the whole phase space [4, 5]. Therefore, one must allow for a Replica Symmetry Breaking (RSB) to construct the solution. Following the Parisi scheme [10], the elements of Q_{ab} can take different values and the order parameter is their probability distribution. Identical copies of the system show different amplitude equilibrium configurations, as the ergodicity is broken in many distinct states.

Four different regimes are found for the photonic system varying parameters $\mathcal{P}$, α, α_0 and R_J:

- *Incoherent Wave (IW):* replica symmetric solution with all order parameters equal to zero. The modes oscillate incoherently and the light is emitted in the form of a continuous wave.
- *Phase Locking Wave (PLW):* all order parameters vanish but r_d, signaling a locking of the mode phases on a line but without a specific direction. This regime occurs in the region of the phase space intermediate between the IW and RL regimes.
- *Mode Locking Laser (ML):* solution with $m \neq 0$, with or without replica symmetry breaking. The modes oscillate coherently with the same phase and the light is emitted in form of pulses.
- *Random Laser (RL):* the modes do not oscillate coherently in intensity, so that $m = 0$, but the overlap matrices Q_{ab} and R_{ab} have a nontrivial structure.

Two typical phase diagrams are shown in Fig. 3. Consider the common experimental situation with an increasing pumping rate $\mathcal{P}$ at fixed R_J, α and α_0. Then:

- for R_J not too large a transition between the IW and the ML regimes is observed increasing the pumping. The transition is robust with respect to the introduction of small disorder;
- for systems with intermediate disorder, the high pump regime remains the ordered ML regime, but the intermediate, partially coherent, PLW regime appears between ML and IW;
- for large R_J, a further transition from ML to RL is observed at high $\mathcal{P}$. Moreover, if R_J exceeds a threshold the ML disappears and the only high pumping phase remains the RL.

This scenario is rather general and remains valid for different values of α and α_0 [4, 5]. The value of α_0 affects the transition toward the ML regime: for high α_0 the transition is discontinuous. On the contrary, if α_0 is low, there are regions in the phase diagram where the transition is continuous. The value of α controls the transition to the RL regime. For $\alpha > \alpha_{\rm nl}$ ($\simeq 0.6297$ for $\epsilon = 1$) the transition is toward a RL via a *random first order transition*, typical of glassy systems, with a region of finite complexity antecedent the transition (cf. Fig. 3(a)) where the photonic glass has an exponential number of metastable states corresponding to different mode locking processes.

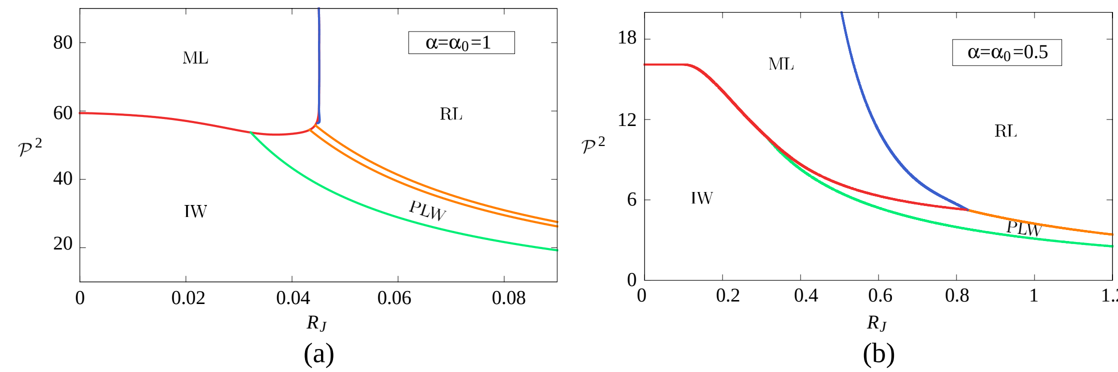

Figure 3: Phase diagram for $\epsilon = 1$ and (a) $\alpha = \alpha_0 = 1$, corresponding to a closed cavity, and (b) $\alpha = \alpha_0 = 0.5$. The solid (dashed) line between IW and ML corresponds to a continuous (discontinuous) transition. The dashed line between PLW and RL in (a) indicates the dynamic transition line with finite complexity.

4. CONCLUSIONS

We have presented statistical mechanical models for ordered and disordered multimode lasers in closed and open cavities. The approach uses equilibrium statistical mechanics tools to study the steady-state of the system via the introduction of an effective temperature.

Monte Carlo simulations for a model for passive mode locking show that the interaction network becomes inhomogeneous for high finesse, resulting in the appearance of phase waves and a nontrivial carrier-envelop phase delay in the pulsed regime. The analysis shows several other properties of experimental relevance: narrowing of the intensity spectrum, vanishing two-mode correlators, optical bistability, robustness against small homogeneous dilution while a non-equipartited condensation appears for large dilution [2, 3].

A general mean-field model for light wave systems in optically active random media is solved via the replica method. The most general phase diagram, ranging from ordered closed cavities (standard lasers) to disordered open cavities (RLs) furnishes a number of different equilibrium phases determined by nonlinearity and disorder. These include passive mode locking in standard lasers, and different coherent regimes attainable in RLs. An experimental test for the RSB predicted by this theory at the RL threshold has been put forward in Ref. [11]: the symmetry breaking in the intensity fluctuation overlap is shown to be equivalent to the one occurring in the complex amplitude overlap, proposing a test directly for shot-to-shot intensity spectra. This result establishes that the intensity fluctuations analysis of Ref. [12] is the first experimental evidence of RSB.

ACKNOWLEDGMENT

This research has received funding from the People Programme of the European Union's Seventh Framework Programme FP7/2007-2013/ under REA grant agreement No. 290038, NETADIS project, from the ERC grant agreement No. 247328 — CriPheRaSy project — and from the Italian MIUR under the Basic Research Investigation Fund FIRB2008 program, grant No. RBFR08M3P4, and under the PRIN2010 program, grant code 2010HXAW77-008.

REFERENCES

1. Gordon, A. and B. Fisher, *Phys. Rev. Lett.*, Vol. 89, 103901, 2002.
2. Antenucci, F., M. Ibáñez Berganza, and L. Leuzzi, *Phys. Rev. A*, Vol. 91, 043811, 2015.
3. Antenucci, F., M. Ibáñez Berganza, and L. Leuzzi, arXiv: 1412.8610, 2015.
4. Antenucci, F., C. Conti, A. Crisanti, and L. Leuzzi, *Phys. Rev. Lett.*, Vol. 114, 043901, 2015.
5. Antenucci, F., A. Crisanti, and L. Leuzzi, *Phys. Rev. A*, Vol. 91, 053816, 2015.
6. Viviescas, C. and G. Hackenbroich, *Phys. Rev. A*, Vol. 67, 013805, 2003.
7. Cao, H., et al., *Phys. Rev. Lett.*, Vol. 82, 2278, 1999.
8. Wiersma, D. S. and S. Cavalieri, *Nature*, Vol. 414, 708, 2001.
9. Marruzzo, A. and L. Leuzzi, *Phys. Rev. B*, Vol. 91, 054201, 2015.
10. Mézard, M., G. Parisi, and M. A. Virasoro, *Spin Glass Theory and Beyond*, 1987.
11. Antenucci, F., A. Crisanti, and L. Leuzzi, arXiv: 1412.8748, 2015.
12. Ghofraniha, N., et al., *Nature Communications*, Vol. 6, 6058, 2015.